

Intermolecular Hydrogen Bond Vibrations

Aleksander Novak

Laboratoire de Spectrochimie Infrarouge et Raman C.N.R.S., 2 rue Henri Dunant, 94320 — Thiais, France

Received December 7, 1981

A few aspects of intermolecular hydrogen bond vibrations are discussed. The methods of assignment of $AH \cdots B$ stretching and bending modes depend considerably on the physical state as shown for some carboxylic acids, phenols and alcohols, nitrogen bases, and acid salts. A number of hydrogen bond stretching frequencies and force constants are given and their correlation with AH stretching frequencies is discussed. The role of $AH \cdots B$ vibrations in determining the breadth and the structure of the AH stretching band is analysed. Finally, the behaviour of the $\nu OH \cdots O$ Raman bands during the phase transition of crystals of squaric acid and cesium dihydrogen phosphate is described.

INTRODUCTION

When a hydrogen bonded $AH \cdots B$ complex or $(AH)_2$ cyclic dimer is formed rotations and translations of AH and B molecules are transformed into vibrational modes usually called hydrogen bond vibrations. There are frequently six such vibrations; however, there may be more or less of them depending on the type of the hydrogen bonded system and the symmetry of the donor and acceptor molecules. Hydrogen bond stretching ($\nu AH \cdots B$ or ν_σ) and bending ($\delta AH \cdots B$ and $\gamma AH \cdots B$) vibrations can be distinguished the former being particularly interesting. The hydrogen bond vibrations are of great interest since they can provide direct information concerning the force constants of the hydrogen bond, they may be used for testing the potential function connected with breaking of the hydrogen bond¹, and are indispensable for the calculation of the equilibrium association constants. Furthermore, they play an important role in determining the AH stretching band profile which has been extensively discussed in the literature²⁻⁶.

Because of the relative weakness of hydrogen bond force constants of these modes are small and the resulting frequencies are thus low, usually lower than 300 cm^{-1} , i. e. in absorption they fall in the far infrared region and in Raman scattering close to the exciting line. The corresponding instrumental difficulties were gradually overcome and for the last fifteen years or so the hydrogen bond vibrations can be examined with commercial apparatus both in infrared and in Raman. However, there are some intrinsic difficulties in studying these vibrations since other intramolecular or lattice vibrations can give rise to low-frequency bands and in some cases a coupling between intramolecular and hydrogen bond vibrations occurs.

* Festschrift of Professor Dušan Hadži.

The aim of this paper is to discuss some aspects of hydrogen bond vibrations, such as assignment problem, force constants, AH stretching band breadth and structure, and structural phase transitions, and not to give a review of the investigated intermolecular modes. Pertinent reviews have already been published by Pimentel and McClellan^{1,6}, Jakobsen et al.⁷, Rotschild⁸ and Wood⁹.

ASSIGNMENT PROBLEM

In order to identify the hydrogen bond frequencies gas and liquid phase studies offer some advantages since the pressure or concentration and temperature variation can be used: the intensity of the corresponding bands is expected to decrease with the decreasing intensity of the associated ν AH band. However, the bands are frequently broad and only rarely all the expected intermolecular vibrations are observed. In the low-temperature crystal spectra, on the other hand, the bands are usually sharp and polarised light measurements of single crystals can help in assignment. Nevertheless, the interpretation of the spectra of hydrogen bonded crystals can be complicated since some lattice vibrations may not involve hydrogen bonds. Finally, isotopic shifts can be used in order to distinguish the rotational and translational vibrations -if there is not too much coupling between them- and thus the hydrogen bond stretching and bending modes. The substitution of the AH acidic hydrogen by deuterium is of course not sufficient but well measurable shifts are expected for totally deuterated derivatives such as CD_3COOD , $\text{C}_2\text{D}_3\text{ND}$, $\text{C}_5\text{D}_5\text{NDCl}$, $\text{N}_2\text{D}_5\text{Cl}$ or for ^{18}O substituted compounds such as oxalic acids and acid oxalates or phosphates.

Carboxylic Acids

Because of the strength of association, intermolecular modes were first observed in the carboxylic acid dimers^{10,11} which are among the most extensively investigated compounds¹²⁻³². It has been well established in both formic and acetic acid^{12,15,18}, which form cyclic dimers of the effective C_{2h} point group symmetry in vapour phase, that the three infrared active hydrogen bond vibrations can be described as $\text{OH}\cdots\text{O}$ stretching, the $\text{OH}\cdots\text{O}$ out-of-plane bending, and the ring torsional modes; they can be considered as rotational vibrations (R') of the monomers. The three Raman active modes, on the other hand, are identified as ν $\text{OH}\cdots\text{O}$, δ $\text{OH}\cdots\text{O}$, and γ $\text{OH}\cdots\text{O}$ vibrations and are derived from one translational T' and two rotational vibrations R' of the monomers. The frequencies and the assignment of formic and acetic acid together with those of trifluoroacetic and benzoic acids are given in Table I. The forms of the three out-of-plane hydrogen bond vibrations are shown in Figure 1. It is interesting to note that the γ $\text{OH}\cdots\text{O}$ mode of B_g species has the highest frequency⁷ unlike most of the other self-associated carboxylic acids for which the highest external frequency corresponds to a ν $\text{OH}\cdots\text{O}$ vibration. Another interesting feature is the appearance of the 188—168 cm^{-1} doublet of acetic acid dimer which has been interpreted in terms of a Fermi resonance between the ν $\text{OH}\cdots\text{O}$ fundamental near 188 cm^{-1} and γ $\text{OH}\cdots\text{O}$ (130 cm^{-1}) + twist (50 cm^{-1}) combination⁷ and cannot be ascribed to proton tunnelling¹⁷.

The spectra of propanoic and higher acids become more complicated since some skeletal bending modes give also rise to low-frequency bands. However, in some cases the hydrogen bond and intramolecular vibrations can be disting-

uished using isotopic shifts: in the spectrum of propanoic acid, for instance, two bands at 169 and 121 cm^{-1} shift to 150 and 100 cm^{-1} for $\text{CD}_3\text{CD}_2\text{COOD}$ species yielding isotopic frequency ratio of 1.13 and 1.21, respectively. The former is consistent with a hydrogen bond stretching vibration of rotational

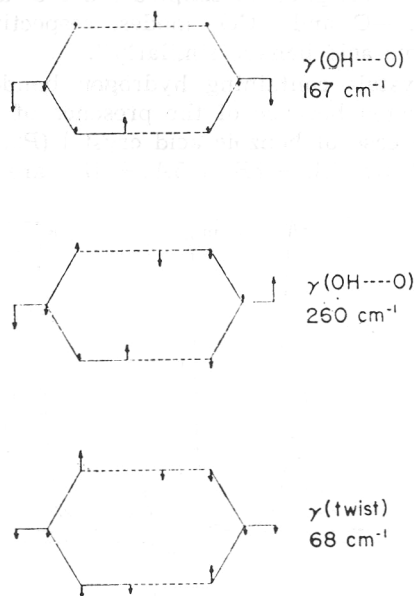


Figure 1. Cartesian displacements of out-of-plane hydrogen bond vibrations of formic acid¹⁷.

TABLE I

Hydrogen Bond Frequencies of Some Carboxylic Acids (Cyclic Dimers)

Approximate type of motion ^a	Symmetry species	$(\text{HCOOH})_2$ gas		$(\text{CH}_3\text{COOH})_2$ gas		$(\text{CF}_3\text{COOH})_2$ solid ²³ gas ²²		$(\text{C}_6\text{H}_5\text{COOH})_2$ solid ^{24,25}	
		calc. ¹²	obs. ^{15,31}	calc. ^{15,32}	obs. ^{15,18}				
$\nu \text{OH}\cdots\text{O}$ R'_z	B_u	248	248	187	188, 168 ^c	146	154	A_u	B_u ^b
								104	106
$\gamma \text{OH}\cdots\text{O}$ R'_x	A_u	160	164	79				62	65
γ twist R'_y	A_u	60	68	54	50	41	34	86	76
								A_g	B_g ^b
$\gamma \text{OH}\cdots\text{O}$ R'_x	B_g	243		130		92		93	96
$\nu \text{OH}\cdots\text{O}$ T'_y	A_g	222	230 ± 5	210				122	126
$\delta \text{OH}\cdots\text{O}$ R'_z	A_g	103		81				114	114

^a R'_x , R'_y , and R'_z are the rotational vibrations of monomers about the axes of the principal moments of inertia I_x , I_y , I_z .

^b Factor group splitting due to the presence of two dimers in the unit cell.

^c Fermi resonance doublet.

origin while the latter is too high for an external motion and is assigned to a torsional τ C—C mode⁷. In other cases, low frequency intramolecular vibrations can be strongly coupled with hydrogen bond vibrations as shown by Suzuki and Shimanouchi^{20,21}: three infrared bands of succinic acid crystal at 225, 149, and 98 cm^{-1} are assigned to coupled δ C'C'C' and ν OH \cdot O, τ C'—C' and δ OH \cdot O, and τ C'—C and τ CO₂ modes, respectively²⁰. The hydrogen bond vibrations of adipic acid behave similarly²¹.

The spectra of crystals containing hydrogen bonded carboxylic dimers can be further complicated because of the presence of more than one dimer in the unit cell. In the case of benzoic acid crystal ($P2_1/c$, $Z = 4$) 21 external vibrations, represented by $6A_g + 6B_g + 5A_u + 4B_u$ are expected. There are

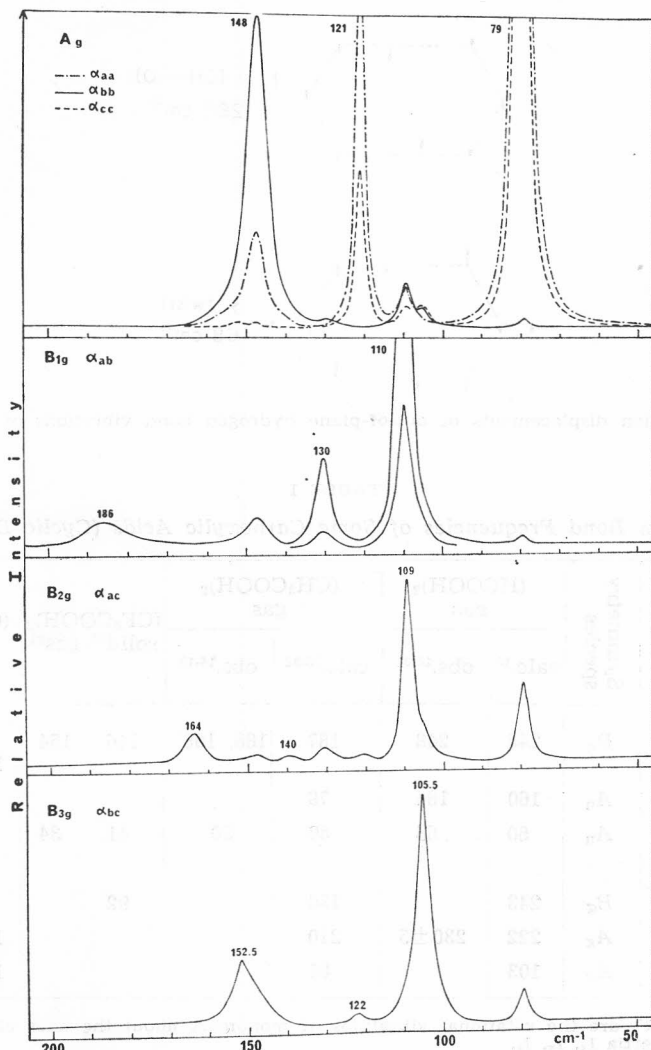


Figure 2. Polarised low-frequency Raman spectra of α -oxalic acid ($\text{H}_2\text{C}_2\text{O}_4$) single crystal at 300 K; after reference²⁹.

twelve hydrogen bond vibrations, six for each dimer, and nine lattice modes which correspond to rotational and translational vibrations of cyclic dimers as a whole and thus do not involve hydrogen bonds^{24,25}. The frequencies of the latter are all below 80 cm⁻¹.

A special problem is posed by the low-frequency spectra of anhydrous, α and β , oxalic acids^{28,29} which have different crystal structures and hydrogen bonds. These crystals have unusual high density and strong correlation field splitting due not only to hydrogen bonds but also to short intermolecular C··O interactions. As a result the lattice frequencies are rather high (198—84 cm⁻¹) but do not follow the usual pattern of hydrogen bond stretching and bending motions²⁹. In the case of α form (P_{cab} , $Z = 4$), for instance, twelve rotational vibrations are only Raman active and nine translational vibrations are only infrared active the molecules occupying the centers of inversion. All the twelve R' modes have been observed in Raman and are shown in Figure 2: they are all due to hydrogen bond vibrations but so-called ν OH··O, δ OH··O and γ OH··O vibrations are heavily mixed (Table II). The same is true of infrared active T' modes some of which are coupled also with intramolecular τ C—C motions. Moreover, it is significant that the highest lattice frequencies do not correspond to predominantly hydrogen bond stretching vibration, as usually encountered in the spectra of hydrogen bonded crystals, but rather to the motions involving the variation of C··O distances, denoted as (δ OH··O and γ OH··O) or (γ OH··O and ν OH··O)²⁹.

TABLE II
Hydrogen Bond Stretching Frequencies of Some Representative Systems

Compound	Phys. state	Association type	AH··B	Frequency cm ⁻¹	Reference
Methanol	crystal	chains	OH··O	348	34, 35
Ethanol	liquid		OH··O	110	33
Phenol	liquid		OH··O	162	36
3-methylphenol	liquid		OH··O	143	36, 37
4-methylphenol	liquid		OH··O	178, 126*	37, 36
3-chlorophenol	liquid		OH··O	130	37
4-chlorophenol	liquid		OH··O	122	37
	α -crystal	chains	OH··O	183, 175; 186, 173, 170, 160	40
	β -crystal	cyclic tetramers	OH··O	163, 165, 159	40
	γ -crystal		OH··O	178	40
1-naphtol	crystal	chains	OH··O	160	41
<i>Phenol complexes</i>					
Phenol-pyridine	CCl ₄ solution	1 : 1 complex	OH··N	130	38
4-iodophenol-pyridine	CCl ₄ solution	1 : 1 complex	OH··N	115	38
4-nitrophenol-pyridine	C ₆ H ₆ solution	1 : 1 complex	OH··N	137	39
Phenol-triethylamine	CCl ₄ solution	1 : 1 complex	OH··N	123	38

Compound	Phys. state	Association type	AH···B	Frequency cm ⁻¹	Reference
<i>Acids</i>					
Formic	gas	cyclic dimers	OH···O	248, 230	12, 15, 18
	crystal	chains	OH···O	232, 177	15, 19
Acetic	gas	cyclic dimers	OH···O	188, 168 ^b	15, 18
	crystal	chains	OH···O	198	15, 26
Propionic	liquid	cyclic dimers	OH···O	169	7
Butyric	liquid	cyclic dimers	OH···O	154	13
Monochloroacetic (MCA)	crystal	cyclic dimers	OH···O	152	42
Trichloroacetic	crystal	cyclic dimers	OH···O	107	13
Trifluoroacetic	gas	cyclic dimers	OH···O	154	22
	crystal	cyclic dimers	OH···O	146	23
Benzoic	crystal	cyclic dimers	OH···O	126, 122; 106, 104	24, 25
Oxalic	α -crystal	layers	OH···O OH···O	198, 174, 166, 161, 130, 117, 84 ^c	28, 29
	β -phase	chains of cyclic dimers	OH···O OH···O	177, 121, 70 ^c	29
Malonic	crystal	chains of cyclic dimers	OH···O	190 ^a	30
Succinic	crystal	chains of cyclic dimers	OH···O	225 ^a	20
Sulphuric	crystal	layers	OH···O	170	43
	crystal	cyclic dimers	OH···O	203	44
Squaric	crystal	layers	OH···O	234	45, 46
<i>Adducts</i>					
MCA-DMSO ^d	liquid	1:1 complex	OH···O	178	42
TCA-DMSO	liquid	1:1 complex	OH···O	165	42
MCA-TPPO ^d	liquid	1:1 complex	OH···O	128	42
TCA-TPPO	solid	1:1 complex	OH···O	108	42
<i>Acid salts</i>					
KHCO ₃	crystal	cyclic dimers	OH···O	265 ^a ; 232, 222	47, 48
NaHCO ₃	crystal	chains	OH···O	240	44
CsH ₂ PO ₄	crystal (para-electric)	layers	OH···O	234, 219; 220	49

Compound	Phys. state	Association type	AH...B	Frequency cm ⁻¹	References
KH(CH ₃ COO) ₂	crystal	1:1 complex	OH...O	270	50
NaH(CH ₃ COO) ₂	crystal	1:1 complex	O—H—O	320	51
KH(C ₆ H ₅ COO) ₂	crystal	1:1 complex	O—H—O	300	52
KH(C ₆ H ₅ CH ₂ COO) ₂	crystal	1:1 complex	O—H—O	340	52
H ₃ O ₃ ⁺ Cl ⁻	crystal	1:1 complex	O—H—O	440	53
KHF ₂	crystal	(FHF) ⁻	F—H—F	603, 596	54
NaHF ₂	crystal	(FHF) ⁻	F—H—F	630	54
<i>XH complexes</i>					
FH...NCH	gas	1:1 complex	FH...N	197	55
FH...NCCH ₃	gas	1:1 complex	FH...N	181	56
ClH...NCCH ₃	gas	1:1 complex	Cl...HN	100	57
FH...OH ₂	gas	1:1 complex	FH...O	198	58
FH...O(CH ₃) ₂	gas	1:1 complex	FH...O	185	59
ClH...O(CH ₃) ₂	gas	1:1 complex	ClH...O	119	60
<i>Nitrogen bases</i>					
Pyrrole	liquid	polymers	NH...π	110	61
	crystal	chains	NH...π	141, 131; 137	62
Imidazole	liquid	polymers	NH...N	120	63
	crystal	chains	NH...N	179; 172	63, 64, 65, 66
1,2,4-triazole	crystal	chains	NH...N	200; 198	67
Purine	crystal	chains	NH...N	168	68
Adenine	crystal	layers	NH...N	147, 108	69
9-methyladenine	crystal	layers	NH...N	117, 99; 118, 98	70
1-methyluracil	crystal	cyclic dimers	NH...O	123, 100; 97, 82	70
1-methylthymine	crystal	cyclic dimers	NH...O	106; 96, 79	70
N-methylacetamide	crystal	chains	NH...O	130	71
<i>Protonated bases</i>					
Pyridinium chloride	crystal	1:1 complex	NH ⁺ ...Cl ⁻	192	72
Pyridinium bromide	crystal	1:1 complex	NH ⁺ ...Br ⁻	133	72
Pyridinium iodide	crystal	1:1 complex	NH ⁺ ...I ⁻	110	72
Pyrazinium chloride	crystal	1:1 complex	NH ⁺ ...Cl ⁻	186	73
Pyrimidinium chloride	crystal	1:1 complex	NH ⁺ ...Cl ⁻	198	73
Purinium chloride	crystal	1:1 complex	NH ⁺ ...Cl ⁻	196	74

^a νOH...O vibration is coupled with skeletal bending mode(s)

^b Fermi resonance doublet

^c There is no dominant νOH...O mode: all these frequencies correspond to vibrations having some νOH...O character

Alcohols and Phenols

Lake and Thompson³³ studied far-infrared spectra of liquid and solid alcohols and assigned ν OH \cdots O band of liquids mostly in the 145 to 180 cm^{-1} region while the frequencies of solid alcohols were found considerably higher; in the particular case of ethanol the 110 cm^{-1} liquid band is reported to shift to 218 cm^{-1} . Jakobsen et al.⁷, on the other hand, claim that both bands, near 110 and 220 cm^{-1} , are observed in the liquid as well as in the solid spectra. The comparison of the far infrared absorption of a hydrogen bonded compound in the liquid and solid state may not always be safe since the liquid band can correspond to motions different from those in the crystal; furthermore, the type of association can also change as it happens for formic and acetic acid (Table II). A single broad absorption of a (disordered) liquid alcohol may thus correspond to a superposition of different rotational and translational (OH \cdots O stretching and bending) motions while in the (ordered) crystal several narrow bands can be assigned to well-defined lattice modes. The best example is the low-temperature α -methanol crystal studied by Dempster and Zerbi³⁴ and by Wong and Whalley³⁵ who carried out a very careful vibrational analysis of this compound. Among the infrared active lattice modes the 348 cm^{-1} band has been attributed to predominantly OH \cdots O stretching vibration^{34,35}. This mode is strongly dispersed and the ν OH \cdots O motions become strongly mixed with δ OH \cdots O modes (along the ν_{23} branch).³⁴

Similar problems are encountered in the spectra of phenols. The identification of intermolecular hydrogen bond vibrations in the 200 to 100 cm^{-1} region appears firmly established^{7,36-38} by comparing simultaneously the OH stretching and OH \cdots O region using dilution in solvents or polyethylene matrix³⁶ or substituting an $-\text{OCH}_3$ group for $-\text{OH}$ ³⁷. However, since numerous polymeric forms of association are possible in the liquid, the low-frequency band probably represents the superposition of the ν_σ bands of several associated species⁹. Coupling with intramolecular modes has also been shown to exist in the case of para-cresol where the 178 and 126 cm^{-1} bands have been interpreted as mixed ν OH \cdots O and skeletal bending motions³⁶. Solutions of phenols and pyridines (in excess) in CCl_4 yield only 1 : 1 complexes: the resulting ν OH \cdots N bands are narrow, $\nu_{1/2} = 15 \text{ cm}^{-1}$, indicating the presence of a single species^{9,38} (Table II). Crystalline phenols, on the other hand, can give rise to more or less numerous ν OH \cdots O infrared and Raman bands depending on the crystal symmetry and number of molecules in the unit cell. An interesting case is that of 4-chlorophenol giving a single liquid band³⁷ at 122 cm^{-1} while in the solid there are three phases denoted as α , β and γ . α -phase consisting of infinite chains of self-associated molecules was studied as single crystal with polarised light in absorption and in Raman scattering⁴⁰. Two Raman (A_g and B_g) bands at 183 and 175 cm^{-1} have been assigned to ν OH \cdots O vibration of translational (T') and rotational (R') origin, respectively while the infrared counterparts at 186, 173, 170, and 160 cm^{-1} correspond to R' vibrations⁴⁰. β -crystal contains cyclic tetramers and gives rise to a Raman band at 163 cm^{-1} (T') and to two infrared bands at 165 and 159 cm^{-1} (R')⁴⁰. Finally, a single ν OH \cdots O frequency at 178 cm^{-1} has been observed in the spectrum of the γ -phase⁴⁰ the structure of which is not known.

Nitrogen Bases and Protonated Derivatives

Self-associated pyrrole containing $\text{NH} \cdots \pi$ hydrogen bonds is representative of weakly interacting systems and behaves similarly as alcohols and phenols. A broad absorption near 110 cm^{-1} of the liquid⁶¹ is substituted by narrow bands at 141 and 131 cm^{-1} in the crystal⁶². Both are believed to be due to ν_σ the former being a T' and the latter a R' vibration as shown by the isotopic frequency ratios ν/ν' ($\text{C}_4\text{H}_4\text{NH}/\text{C}_4\text{D}_4\text{ND}$) of 1.02 and 1.10 respectively. A Raman R' counterpart ($\nu/\nu' = 1.10$) is observed at 137 cm^{-1} and its intensity is low⁶².

Imidazole crystal consists of infinite chains of molecules linked by medium-strong $\text{NH} \cdots \text{N}$ hydrogen bonds and has been studied by several authors⁶³⁻⁶⁶. It belongs to the $P2_1/c = C_{2v}^{5h}$ space group with four molecules per unit cell: 21 lattice vibrations represented by $6A_g + 6B_g + 5A_u + 4B_u$ are thus expected. Six out of the nine infrared active vibrations have been observed at 179 (A_u, T'), 142 (A_u, R'), 144 (B_u, R'), 103 (A_u, T'), 89 (B_u, T'), and 62 (B_u, R') cm^{-1} and assigned to their symmetry species, using infrared dichroism, and to translational and rotational vibrations, using the isotopic shifts of imidazole- d_4 crystal (Figure 3). The isolated chain approximation was helpful in separating the intrachain (hydrogen bond) vibrations and interchain modes which do not involve hydrogen bond. The 179 and 142 cm^{-1} bands were assigned to predominantly $\nu \text{NH} \cdots \text{N}$ vibrations while the other bands correspond to hydrogen bond bending and torsional motions⁶³. In the Raman spectra of single crystals⁶⁴⁻⁶⁶ ten out of twelve lattice modes have been identified at 172 (B_g, T'), 154 (B_g, R'), 148 (A_g, R'), 114 (B_g, R'), 92 (B_g, R'), 88 (A_g, T'), 77 (A_g, R'), 73 (A_g, T'), 54 (B_g, T'), and 43 (A_g, T'). The bands at 77 and 43 cm^{-1} were attributed to interchain vibrations⁶⁴. The normal coordinate calculations agree with the distinction between intra- and interchain modes and show a predominantly $\nu \text{NH} \cdots \text{N}$ character of the 179 cm^{-1} infrared and 172 cm^{-1} Raman band. The 142 cm^{-1} A_u frequency, on the other hand, is interpreted as a hydrogen bond torsional vibration⁶⁶.

1,2,4-triazole crystal also contains infinite chains of $\text{NH} \cdots \text{N}$ hydrogen bonded molecules but its crystal structure is different ($Pbca = D_{2h}^{15}$) and there are eight molecules per unit cell. A polarised light study of single crystals allowed to assign 32 out of the 39 infrared (15) and Raman (24) active lattice modes which were compared to those calculated on the ground of the rigid body and flexible molecule models assuming appropriate intermolecular atom-atom potentials⁶⁷. Unlike for imidazole crystal the normal coordinate calculations do not confirm much of the one-dimensional chain approximation and the distinction between intra- and interchain modes appears limited: there are only six frequencies out of the thirteen expected from the one-dimensional chain model which can be considered as interchain vibrations. The highest intrachain frequencies at 200 ($B_{2g}, 0.66 T'_z + 0.19 R'_y$), 199 ($B_{3g}, 0.73 T'_z + 0.20 R'_y$) and 198 cm^{-1} ($B_{1u}, 0.75 T'_z + 0.14 R'_y$) are assigned to essentially $\text{NH} \cdots \text{N}$ stretching vibrations. The remaining bands correspond to 21 $\text{NH} \cdots \text{N}$ bending and 2 chain torsional modes⁶⁷.

A similar study has been carried out on purine crystal ($Pna2_1 = C_{2v}^9, Z = 4$): 16 of the 21 expected lattice modes have been observed and assigned⁶⁸. There is a considerable mixing of rotational and translational vibrations, however, there does not appear to be much coupling between internal and external motions in spite of the low-frequency (268 and 230 cm^{-1}) of the former.

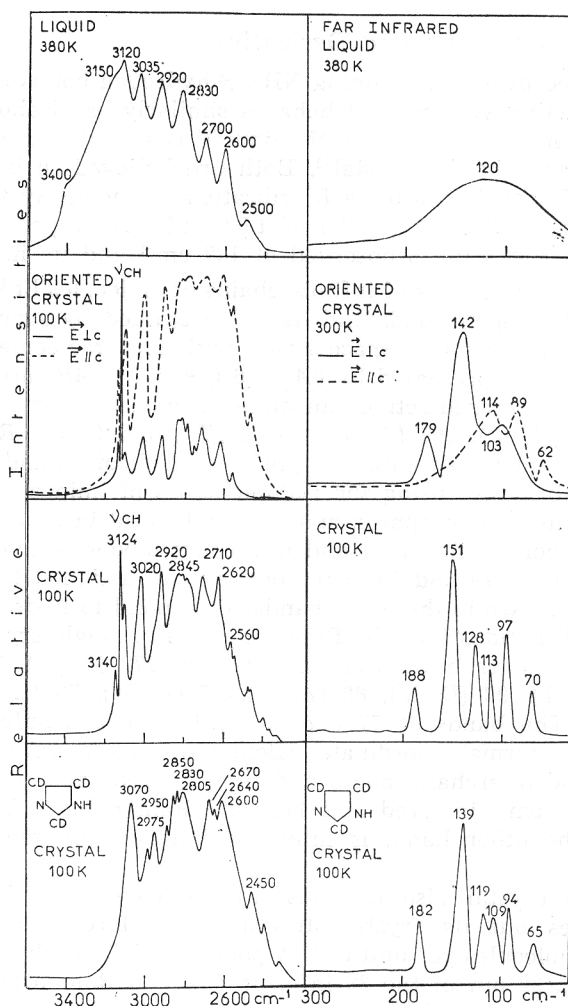


Figure 3. Infrared spectra of imidazole. Near-infrared spectra of (a) liquid at 380 K, (b) oriented crystal at 300 K with electric vector of the incident light perpendicular (—) and parallel (----) to the c axis. (c) polycrystalline sample at 90 K, (d) polycrystalline sample of $C_3D_3N_2H$ deuterated derivative at 90 K. Far-infrared spectra of (e) liquid at 380 K, (f) oriented crystal as in (b), (g) polycrystalline sample at 90 K, (h) $C_3D_3N_2H$ crystal at 90 K. After reference⁴.

The highest lattice frequency observed at 168 cm^{-1} (B_1 , $0.80 T_y' + 0.59 R_x'$) is due to a $NH \cdots N$ stretching mode; the second $\nu NH \cdots N$ vibration of A_2 species calculated at 176 cm^{-1} has not been observed⁶⁸.

Finally, Harada and Lord⁷⁰ have studied the lattice vibrations, by infrared and Raman spectroscopy as well as by normal coordinate calculations, of 1-methyl-thymine, 9-methyladenine, of their 1:1 complex, and of 1-methyl-uracil, which can furnish a basis for the interpretation of biopolymers, such as DNA and RNA¹. They have identified the $NH \cdots N$ stretching frequencies of 9-methyladenine crystal ($P2_1/c$, $Z = 4$) at 118 (B_g), 117 (A_u), 99 (B_u), and 98 cm^{-1} (A_g) and $\delta NH \cdots N$ at 81 (B_u) and 74 (A_g) cm^{-1} . Similar values were

obtained for the $\text{NH}\cdots\text{O}$ frequencies of 1-methylthymine and 1-methyluracil crystals⁷⁰ (Table II).

Protonated nitrogen bases. Pyridinium, pyrimidinium, and pyrazinium halides represent $\text{NH}^+\cdots\text{X}^-$ proton transfer hydrogen bonded compounds with a monoatomic acceptor: the structures and hydrogen bond vibrations of these relatively rigid systems^{72,73} appear thus less complicated than the preceding ones. Pyridinium chloride crystal ($P2_1/m = C_{2h}^2$), for instance, contains two $\text{C}_5\text{H}_5\text{NH}^+\cdots\text{Cl}^-$ complexes in the unit cell giving rise to 15 lattice vibrations: $5A_g + 4B_g + 3A_u + 3B_u$ ⁷². The $\text{NH}^+\cdots\text{Cl}^-$ forces are expected much stronger than those between complexes: »intracomplex« and »inter-complex« lattice modes can thus be distinguished. The latter correspond to translational motions of a complex as a whole ($2A_g + B_g$) and do not involve hydrogen bonds. The former consist of three rotational and three translational vibrations for each complex, i. e. there are $6R'$ ($A_g + 2B_g + 2A_u + B_u$) and $6T'$ ($2A_g + B_g + A_u + 2B_u$) modes.

The far-infrared spectra of pyridinium chloride crystal⁷² show three strong bands at 192, 116, and 92 cm^{-1} and three weak bands at 142, 70, and 50 cm^{-1} (Figure 4). The strong bands shift but little ($\nu/\nu' = 1.01$) on total deuteration of the cation ($\text{C}_5\text{D}_5\text{ND}^+$) and are assigned to translational modes while the weak bands shift much more ($\nu/\nu' = 1.14, 1.09, \text{ and } 1.11$) and correspond thus to rotational motions. The opposite is observed in Raman where the strongest band at 133 cm^{-1} is due to a libration (Figure 4). Similar spectral pattern is observed for pyridinium bromide and iodide⁷² the frequencies of which are given in Table III. The $\text{NH}^+\cdots\text{X}^-$ hydrogen bond strength decreases in going from chloride to bromide and iodide as shown by their increasing NH stretching frequencies (Table III). One would expect, therefore, that the $\text{NH}^+\cdots\text{X}^-$ frequencies decrease in the same series. This is precisely what happens to the translational vibrations which are thus assigned to hydrogen bond modes: the highest T' frequency being the most sensitive towards halogen substitution is a $\text{NH}\cdots\text{X}$ stretching mode and the lower two $\text{NH}\cdots\text{X}$ bending modes. The rotational frequencies, on the other hand, do not show such a trend and vary quite irregularly (Table III): they cannot be considered as hydrogen bond vibrations. This is perhaps not too surprising since only three hydrogen bond vibration of antitranslational type are expected for an isolated $\text{AH}\cdots\text{B}$ complex with monoatomic acceptor. Similar conclusions have been reached for pyrimidinium and pyrazinium halides⁷³.

TABLE III

Lattice and NH Stretching Frequencies of Pyridinium Halides⁷²

Compound	Rotational frequency	Translational (hydrogen bond) frequency			NH stretching frequency ν cm^{-1}	$(\nu_0 - \nu)/\nu_0^a$
		Stretch	Bend			
$\text{C}_5\text{H}_5\text{NH}^+\cdots\text{Cl}^-$	142 70 50	192	116 92	2430	0.27	
$\text{C}_5\text{H}_5\text{NH}^+\cdots\text{Br}^-$	154 66	133	97 88	2800	0.15	
$\text{C}_5\text{H}_5\text{NH}^+\cdots\text{I}^-$	151 70	110	87 75	2990	0.10	

^a $\nu_0 = 3317 \text{ cm}^{-1}$ of »free« pyridinium reineckate.

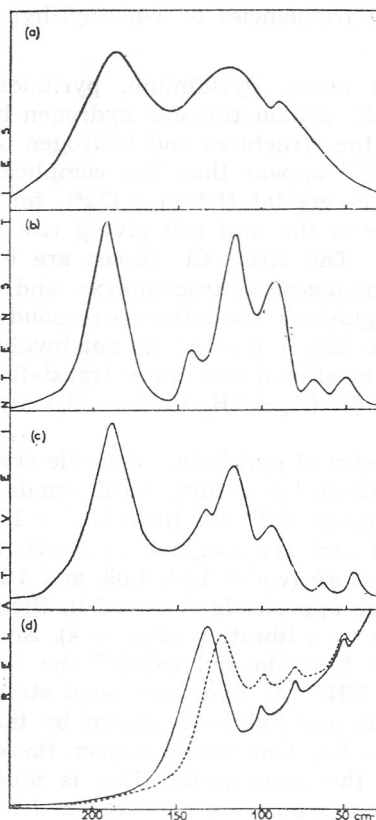


Figure 4. Low-frequency spectra of polycrystalline pyridinium chloride. Far-infrared spectra of (a) $C_5H_5NH^+Cl^-$ at 300 K and (b) at 90 K, (c) $C_5D_5ND^+Cl^-$ at 90 K, Raman spectra of (d) solid line, $C_5H_5NH^+Cl^-$; dotted line, $C_5D_5ND^+Cl^-$, both at 300 K. After reference².

Acid Salts

Acid salts of inorganic and organic acids represent a special class of compounds containing (AHA)⁻ hydrogen bonds, i. e. the acceptor properties of A atoms are equal or very similar. The resulting hydrogen bonds can be symmetric or asymmetric and in any case very strong: in the particular case of (OHO)⁻ system the O...O distances are comprised between 2.60 and 2.40 Å and the OH stretching frequencies between 2600 and 600 cm^{-1} ⁴⁴. The corresponding hydrogen bond stretching frequencies are expected to be high but relatively few compounds have been investigated. A well known example is (FHF)⁻ ion in KHF_2 and $NaHF_2$ crystals containing truly centered hydrogen bonds⁷⁵. For the $NaHF_2$ crystal (D_{3d}^5 , $Z = 3$) the F—H—F symmetric stretching mode (ν_σ) is only Raman active (A_{1g}) and has been identified at 630 cm^{-1} ⁵⁴. The Raman spectrum of KHF_2 (D_{4h}^{18} , $Z = 2$) is more complex and shows two lines at 603 and 596 cm^{-1} assigned to the A_{1g} and B_{2g} species of the F—H—F symmetric stretch⁵⁴. O—H—O analogs are less clear cut: in the case of the symmetrically hydrogen bonded $NaH(CH_3COO)_2$ crystal the ν O—H—O vibration gives rise to a relatively strong Raman band at 320 cm^{-1} ; its isotopic

frequency ratio ($\text{CD}_3\text{COO}/\text{CH}_3\text{COO}$) of 1.09, however, is higher than expected for a pure antitranslational mode and can be due to some coupling with γ CCO vibration⁵¹. Similar ν O—H—O bands near 300 and 340 cm^{-1} have been observed in the Raman spectra of $\text{KH}(\text{C}_6\text{H}_5\text{COO})_2$ and $\text{KH}(\text{C}_6\text{H}_5\text{CH}_2\text{COO})_2$, respectively⁵². Both crystals contain crystallographically symmetrical hydrogen bonds. ν O—H—O frequencies of acid salts with asymmetric hydrogen bonds, on the other hand, are generally lower and have been identified in the 280 to 220 cm^{-1} region (Table II). CsH_2PO_4 crystal ($P2_1/m$, $Z = 2$), for instance, has three ν OH \cdots O vibrations, all of rotational origin: two, at 234 (B_g) and 219 (A_g), have been observed in Raman and one, at 220 cm^{-1} (A_u), in infrared⁴⁹. Finally, KHCO_3 crystal consists of centrosymmetric $(\text{HCO}_3^-)_2$ dimers similar to those of carboxylic acids (Table I) and similar hydrogen bond vibrations are thus expected: in Raman, the antitranslational ν OH \cdots O vibration of A_g species has been found at 222 cm^{-1} and the bending γ OH \cdots O (B_g, R_v') and δ OH \cdots O (A_g, R_w') modes, at 196 and 142 cm^{-1} , respectively⁴⁷. In infrared, the strong 265 cm^{-1} band has been assigned to a ν OH \cdots O mode coupled with a δ CO_3 vibration⁴⁸ while a band near 166 cm^{-1} may be due to an OH \cdots O bending A_u motion⁴⁷.

FORCE CONSTANTS

There are few data on hydrogen-bond stretching force constants and even fewer reliable values. A number of $F_{H..B}$ values is given in Table IV indicating also the calculation methods which range from a crude diatomic molecule approximation (DM) to more or less sophisticated calculations (NCC): among the most reliable values appears to be that of ice since it has been derived from a thorough dynamical calculation which included data from optical spectra and from phonon dispersion curves given by neutron scattering⁷⁶.

One of the questions discussed in earlier literature^{6,7} is whether ν_σ is localised in the triatomic AH \cdots B system or the masses of the two bonded molecules ought to be taken into account. Ginn and Wood³⁸ treated this problem in the case of 1:1 complexes of phenol with a nitrogen base, such as pyridine or trimethylamine, and computed the hydrogen bond force constants using three models: a simplified normal coordinate analysis, triatomic OH \cdots N model (all force constants except those of ν_σ and ν OH are set equal to zero), and the diatomic molecule model, PhOH \cdots N(CH₃)₃ (all force constants except that of ν_σ have been set equal to infinity). The OH \cdots N stretching force constant derived from the DM model (45 Nm^{-1}) is much closer to the value obtained by simplified normal coordinate treatment (27 Nm^{-1}) than that from OH \cdots N group which is much too low (9 Nm^{-1}). The DM model is thus of some usefulness in assigning the hydrogen bond stretching frequencies, in particular if there is but little coupling with intramolecular vibrations and if the ν_σ vibration corresponds to an essentially anti-translational motion. Similar considerations may be applied to a number of self-associated phenols for which a plot of ν_σ versus $M^{-1/2}$ (molecular weight of phenol) yields a straight line³⁶.

Carboxylic acid dimers containing OH \cdots O hydrogen bonds of similar strength appear to have relatively converging values of $F_{H..O}$ ranging from 29 to 36 Nm^{-1} (Table IV). Formic acid dimer was studied by different authors^{12,32,76,77} and the most recent values, close to 30 Nm^{-1} , have been obtained by normal coordinate⁷⁶ as well as by ab initio calculations⁷⁷. The

TABLE IV
 Hydrogen-bond stretching force constants

Compound	Physical state	AH...B	Force constant Nm ⁻¹	Calculation method ^a	Reference
Water	I h Crystal	OH...O	20	DM	6
			29	b)	76
Methanol	α -crystal	OH...O	34.6	NCC	35
			33.2	NCC	34
Phenol-trimethyl-amine complex	CCl ₄ solution	OH...N	27	NCC	38
			44	DM	38
Phenol-pyridine complex	CCl ₄ solution	OH...N	23	NCC	38
			45	DM	38
Formic acid	Gas	OH...O	29	NCC	76
			33	NCC	12
			36	NCC	32
			30.8	c)	77
Acetic acid	Crystal	OH...O	24	NCC	19
	Gas	OH...O	33	NCC	12
			27	DM	44
Benzoic acid	Crystal	OH...O	35	NCC	25
Oxalic acid	α -crystal	OH...O	19.3	NCC	29
Succinic acid	Crystal	OH...O	36	NCC	20
Adipic acid	Crystal	OH...O	36	NCC	21
(CH ₃) ₂ AsOOH	Crystal	OH...O	84	DM	44
KHCO ₃	Crystal	OH...O	76	NCC	48
			46	DM	44
NaHCO ₃	Crystal	OH...O	52	DM	44
KH(CH ₃ COO) ₂	Crystal	OH...O	109	DM	44
NaH(CH ₃ COO) ₂		OH...O	178	DM	44
HF · CH ₃ CN	Gas	FH...N	20	NCC	56
HF · HCN	Gas	FH...N	22.5	NCC	55
Pyrrole	Crystal	NH... π	20	DM	62
Imidazole	Crystal	NH...N	35	DM	78
			68	NCC	66
			38	d)	78
1,2,4-triazole	Crystal	NH...N	35	NCC	67
			41	DM	68
Purine	Crystal	NH...N	36	NCC	68
9-methyladenine (MA)	Crystal	NH...N	11 (k ₁)	NCC	70
1-methylthymine (MT)	Crystal	NH...O	14.5 (k ₂)		
			27 (k ₁)	NCC	70
MA-MT complex	Crystal	NH...O	14 (k ₂)		
			18 (k ₁)		
			18 (k ₂)	NCC	70
N-methylacetamide	Crystal	NH...N	9.5 (k ₃)		
			10	NCC	71
			10		
Pyridinium chloride	Crystal	NH ⁺ ...Cl ⁻	53	DM	72
Pyridinium bromide	Crystal	NH ⁺ ...Br ⁻	42	DM	72
Pyridinium iodide	Crystal	NH ⁺ ...I ⁻	35	DM	72
Pyrimidinium chloride	Crystal	NH ⁺ ...Cl ⁻	57	DM	73
Pyrazinium chloride	Crystal	NH ⁺ ...Cl ⁻	50	DM	73

^a DM = diatomic molecule approximation; NCC = normal coordinate calculations.

^b derived from dynamical calculation using data from optical spectra and from phonon dispersion curves from neutron scattering.

^c Ab initio calculated (9/4 basis set) force constant.

^d modified CNDO/2 calculations.

force constant of the crystal containing infinite HCOOH chains, on the other hand, is lower (24 Nm^{-1})¹⁹ which may seem surprising as the $\nu \text{ OH}$ frequency and $\text{O}\cdots\text{O}$ distance are considerably smaller than those of the gaseous dimer. However, as Mikawa et al¹⁹ pointed out, the hydrogen bond stretching vibration always contains a contribution from the repulsive force between C and H in $\text{H}\cdots\text{O}=\text{C}$; in other words, the interaction between the adjacent molecules in the crystal involves not only the hydrogen bond, but also the repulsive forces. An even more complicated situation is encountered in α -oxalic acid crystal: the lattice as well as some internal vibrations are influenced not only by $\text{OH}\cdots\text{O}$ hydrogen bond but also by very short $\text{C}\cdots\text{O}=\text{C}$ interactions, possibly of charge transfer type, quadrupole-quadrupole, and $\text{C}=\text{O}$ dipole-dipole interactions^{28,29}. The corresponding $\text{OH}\cdots\text{O}$ stretching force constant of 19.3 Nm^{-1} (Table IV) appears too low, when compared to the OH stretching frequency at 3126 cm^{-1} , if only hydrogen bonds were involved.

Nitrogen bases such as imidazole, triazole, and purine crystals contain medium-strong $\text{NH}\cdots\text{N}$ hydrogen bonds similar to the $\text{OH}\cdots\text{O}$ bonds of carboxylic acids, with the $\nu \text{ NH}$ frequency in the 2730 to 2800 cm^{-1} region⁴⁴. The normal coordinate calculations of 1,2,4-triazole based on 32 experimental lattice frequencies give an overall $\text{NH}\cdots\text{N}$ stretching force constant of 35 Nm^{-1} ⁶⁷. This force constant may be further decomposed into $\text{H}\cdots\text{N}$ interaction of 20 Nm^{-1} and $\text{N}\cdots\text{N}$ interaction of 8 Nm^{-1} . The remainder represents the long range interactions in the chain⁶⁷. The value for purine is very similar⁶⁸ while that of imidazole, also obtained from lattice frequencies by NCC, is twice as large (68 Nm^{-1})⁶⁶. This appears much too high and not consistent with the NH stretching frequency (2800 cm^{-1}) and $\text{N}\cdots\text{N}$ distance (2.86 \AA) of imidazole. It may be pointed out that with this value of $F_{\text{H}\cdots\text{N}}$ the $\nu \text{ NH}\cdots\text{N}$ vibration has been calculated at 240 cm^{-1} (A_u) and 248 cm^{-1} (B_g), an overestimate of about 70 cm^{-1} or almost 40% (Table II). The modified CNDO/2 calculations, on the other hand, give 38 Nm^{-1} ⁷⁸ which is not far from the value obtained by a DM approximation (35 Nm^{-1}) and thus similar to those of triazole and purine (Table IV). The $\text{NH}\cdots\text{N}$ and $\text{NH}\cdots\text{O}$ stretching constants of 9-methyladenine, 1-methylthymine, and of their 1:1 complex are lower (Table IV) as expected on the ground of higher NH stretching frequencies.

In the protonated nitrogen bases such as pyridinium halides containing $\text{NH}^+\cdots\text{X}^-$ hydrogen bonds the $\text{NH}\cdots\text{X}$ stretching vibration corresponds to pure antitranslational motion. i. e. it is not mixed with either internal or other external vibrations⁷². There is thus a simple relationship between $\text{NH}^+\cdots\text{X}^-$ and NH stretching frequencies (Table III), and the DM model for the $F_{\text{H}^+\cdots\text{X}^-}$ force constant determination appears satisfactory. The values reported in Table IV may seem high compared to the relative shift of the NH frequency: $F_{\text{H}^+\cdots\text{I}^-}$ of pyridinium iodide (35 Nm^{-1}), which shows a $\nu \text{ NH}$ relative shift of 10% is similar to that of acetic acid, the $\nu \text{ OH}$ relative shift of which is about 20% ⁴⁴. However, it should be borne in mind that these are ionic proton-transfer hydrogen bonds in pyridinium halides and ion-ion interaction can contribute significantly to the force constant values. This is shown in Figure 5 where $F_{\text{H}^+\cdots\text{X}^-}$ force constants are plotted as a function of the NH stretching frequency relative shift: a fairly linear correlation is found⁷³. When the linear relation is extrapolated to $\Delta \nu/\nu_0 = 0$, the value of $F_{\text{H}^+\cdots\text{X}^-}$

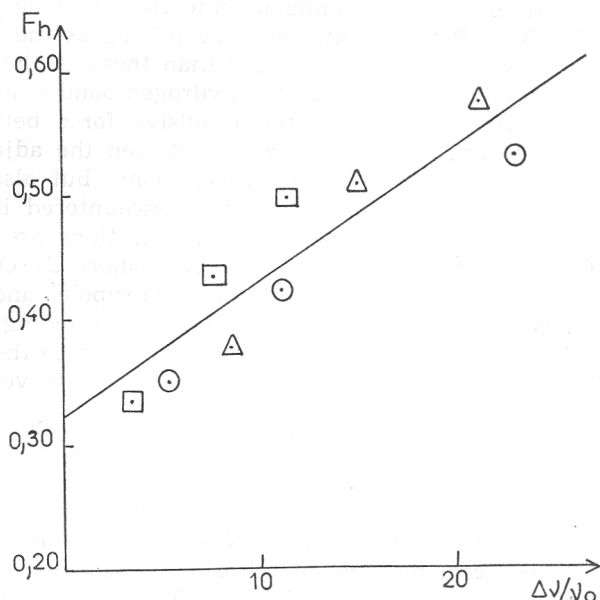


Figure 5. $\text{NH}^+ \dots \text{X}$ hydrogen bond stretching force constant versus relative shift ($\Delta\nu/\nu_0$) of the NH stretching frequency plot.

(circles) Pyridinium halides; (triangles) pyrimidinium halides; (squares) pyrazinium halides. After reference⁹.

is not zero, but 32 Nm^{-1} . This agrees well with the interionic force constants, for $\text{C}_5\text{H}_5\text{NCH}_3^+\text{Cl}^-$ (33 Nm^{-1}) and $\text{C}_5\text{H}_5\text{NCH}_3^+\text{I}^-$ (30 Nm^{-1}) in which there is no hydrogen bonding, obtained using the same model. This value represents the residual Coulomb attraction, arising from the formal charges⁹.

In conclusion, it may be stated that we still need a sufficient number of accurate hydrogen bond stretching force constants, such as determined for ice, methanol, or some carboxylic acids, in order to be able to discuss general correlation with $\nu \text{ AH}$ frequencies or enthalpies of hydrogen bond. Such correlations may be expected for the systems where hydrogen bond is the exclusive or predominant interaction as it probably occurs for gaseous complexes and for complexes with strong hydrogen bonds. However, in the crystals with weak or mediumstrong hydrogen bonds other types of molecular interactions may profoundly influence the $F_{\text{H}\dots\text{B}}$ values. A simple $F_{\text{H}\dots\text{B}} - \nu \text{ AH}$ correlation which would comprise hydrogen bonded gases, liquids, and solids is thus not likely to be found.

AH STRETCHING BAND PROFILE

The role of the low-frequency hydrogen bond vibrations in determining the breadth and the more or less complicated structure of the $\nu \text{ AH}$ band has been extensively discussed in the literature¹⁻⁵. Batuev⁷⁹ was the first to suggest that the subband frequencies can be represented by the expression $\nu = n \pm pN$ where $n = \nu \text{ AH}$, $p = 0, 1, 2 \dots$, and N any hydrogen bond frequency^{79,80}. More sophisticated quantitative theories were developed later, in particular by Maréchal and Witkowski⁸¹ and by Bratos⁸². Their theories

have much in common since n, N coupling is treated in a basically similar way while the divergencies concern mainly the interpretation of the band structure³.

Experimental evidence about the n, N modulation as a structure determining factor is rather different for gases⁸³ and condensed phase⁴. The infrared spectra of complexes of ethers with hydrogen halides and some other complexes in gas phase⁸³ show a ν AH absorption with a central maximum which is accompanied on both sides by weaker submaxima at very similar distances. They have been assigned to ν AH \pm ν AH \cdot B sum and difference combinations due to anharmonic n, N coupling^{83,84}. A detailed study of the temperature dependence of the band intensities of $(\text{CH}_3)_2\text{O} \cdot \text{HCl}$ leads to the conclusion that the highest frequency corresponds to the ν ClH + ν ClH \cdot O combination while the lower frequency shoulder is the ν ClH fundamental^{85,60}. Submaxima due to hydrogen bond bending mode (δ ClD \cdot O) have also been observed in the spectra of ClD \cdot O $(\text{CH}_3)_2$ ⁸⁵ where the spacing is only about 50 to 60 cm^{-1} . Finally, a most notable investigation by Thomas^{57,59} of complexes between HCl or HF and nitriles has led to the observation of another type of subbands: the ν ClH band of ClH \cdot NCCH₃ complex, for instance, consists of a series of sharp peaks superimposed on the broad absorption. The temperature and isotopic study of this band allowed to interpret the structure in terms of hot bands arising from the excited levels of the degenerate hydrogen bond bending vibration⁵⁷, which can be represented by the relationship ν AH + p δ AH \cdot N — p δ AH \cdot N. The frequency of the bending mode is obtained from the subband intensities. The hydrogen bond bending modes of FH \cdot OH₂ complex of C_{2v} symmetry, on the other hand, are not degenerate: the ν FH band fine structure is due to two series of hot bands with different spacings associated with the δ FH \cdot O and γ FH \cdot O vibrations⁸⁶.

The submaxima of the ν ClH band of ClH \cdot O $(\text{CH}_3)_2$ complex in gas phase assigned to N mode progression, disappear in solution and a single band, broader than in gas, is observed. This behaviour corresponds well to theoretical prediction: the N mode is coupled to the thermal bath and its damping is strong enough to blur out the progression of combination bands. This can be generalised by saying that for solution the n, N coupling appears to be the main factor determining the band-width but it has not yet been possible to observe band progression which can be unambiguously assigned to combinations between the n and N modes⁴.

Much the same is true of the solid state and the ν AH band structure can be explained⁴ by Fermi resonances between n fundamental and combinations or overtones of other intramolecular vibrations (n'), mostly δ AH and γ AH modes, ($n, 2n'$ coupling), crystal field splitting (n, n coupling) or strong n, n' coupling⁸⁷.

An example showing clearly that the complex ν AH band structure is not due to hydrogen bond vibrations is given by imidazole. Figure 3 shows near- and far-infrared spectra of this compound and the following comparisons can be pointed out: (a) there are six far-infrared bands assigned to hydrogen bond vibrations (see p. 155); three of them are parallel (B_u) and three perpendicular (A_u) while the ν NH subbands have the same polarisation; (b) when the CH groups are substituted by CD groups some ν NH subbands shift much more than the lattice modes under the same conditions; moreover, the

ν NH structure of $C_3H_3N_2H$ and $C_3D_3H_2H$ are appreciably different; (c) six narrow and well-defined lattice bands of the crystal at 100 K merge into a single broad absorption centered near 120 cm^{-1} when the crystal is melted while there is but little variation of ν NH subbands and essentially the same submaxima persist in the spectrum of the liquid; (d) the relative intensity of the subbands on the low-frequency side increases with decreasing temperature whereas the opposite is expected for the difference bands. The interpretation of subbands as being due to combinations of NH bending and four in-plane skeletal stretching mutually coupled modes, on the other hand, appears satisfactory and explains the shifts of the subbands on different isotopic substitution and as a function of temperature, solvent or physical state⁴. Similar conclusions have been reached for a number of hydrogen bonded crystals⁸⁸ such as triazole⁶⁷, purine⁸⁹, acetic⁸⁸ and oxalic acid²⁸, for instance.

It may be concluded that the anharmonic n, N coupling represents the main band shaping mechanism as far as the band breadth is concerned but not necessarily its structure: the N progression has been observed in the spectra of some complexes in gaseous state but not in those in condensed state.

STRUCTURAL PHASE TRANSITIONS

Hydrogen bond vibrations are, like other lattice vibrations, sensitive towards phase transitions, however not much is known about their specific behaviour during the transformation, not even in the particular case of ferroelectric crystals in which protons engaged in hydrogen bonds obviously play a decisive role. We are reporting here two cases where hydrogen bond vibrations could give interesting information: squaric acid and cesium dihydrogen phosphate.

Squaric acid. Squaric acid is a two-dimensional ferroelectric, consisting of infinite layers of strongly hydrogen bonded ($O\cdots O = 2.53\text{ \AA}$) planar $H_2C_4O_4$ molecules, which undergoes an order-disorder phase transition at 370 K ($D_2C_4O_4$ at 520 K)⁹⁰. The low-temperature phase ($P2_1/m$, $Z = 2$) is ordered while the high-temperature phase ($I4/m$, $Z = 1$) is disordered⁹¹. Vibrational studies of this crystal^{45,46} have shown that the lattice vibrations obey the selection rules derived from the above space groups and Z and see the crystal symmetry much in the same way as x-ray and neutron diffraction. This is not the case of intramolecular vibrations which indicate that the symmetry and the structure of the $H_2C_4O_4$ molecule is the same in both phases and that the $OH\cdots O$ hydrogen bond remains strong and asymmetric above T_c ⁴⁶.

Among nine lattice vibrations of the antiferroelectric ordered phase ($3A_g + 3B_g + 2A_u + B_u$) only rotational ($A_g + 2B_g + 2A_u + B_u$) vibrations can be considered as hydrogen bond vibrations while the three T' modes ($2A_g + B_g$) correspond to interlayer motions. The rotational modes have been observed in Raman⁴⁵ at 244, 156 and 152 cm^{-1} and in infrared⁴⁶ at 230 and 125 cm^{-1} . The 244 and 230 cm^{-1} frequencies can be assigned to $\nu OH\cdots O$ vibrations derived from in-plane librations of A_g and B_u species, respectively, the other frequencies being $OH\cdots O$ bending modes. In the paraelectric disordered phase only two lattice frequencies at 231 (A_g) and 149 cm^{-1} (E_g) are observed in Raman and none in infrared as expected from the selection rules. The 231 cm^{-1} Raman band is thus the only hydrogen bond vibration which can be examined over a wide temperature range in both phases. Figure 6 shows the

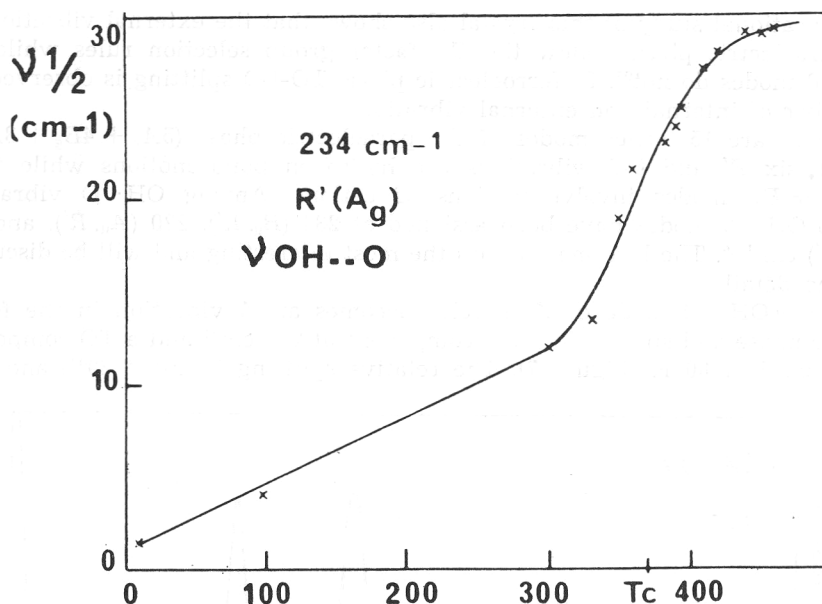


Figure 6. Half-width ($\nu_{1/2}$) of the hydrogen bond stretching Raman band of squaric acid as a function of temperature: T_c -temperature of the phase transition. After reference⁴⁶.

results concerning the $\nu_{1/2}$ half-width of this Raman line in the 10 to 500 K range. The band-width increases drastically in the vicinity of the transition temperature T_c while at higher or lower temperature the variation is smaller. These changes can be qualitatively interpreted using the theory for order-disorder given by Andrade and Porto⁹²: the linear parts of the curve correspond to the band broadening due to vibrational anharmonicity in one potential well while the exponential part near T_c is related to proton jumps from one well to the other according to correlation time $\tau = \tau_0 e^{U/kT}$. It should be pointed out that the $\nu_{1/2}$ variation is considerably larger for the ν OH...O mode (A_g, R') and amounts to about 18 cm^{-1} than for the ν C—C vibration (5 cm^{-1}), for instance. The hydrogen bond stretching vibration modulates directly the O...O distance and can thus influence the proton jumps by the variation of U-activation energy while the skeletal stretching motion perturbs the hydrogen bond much less.

CsH_2PO_4 . The structure of CsH_2PO_4 consists of layers of hydrogen bonded phosphate groups. There are two crystallographically non-equivalent hydrogen bonds: the shorter bond (2.48 Å) links the phosphate groups into the chains along b (polar) axis while the longer bond (2.54 Å) crosslinks the chains into layers⁹³. A pseudo-one-dimensional paraelectric-ferroelectric phase transition occurs at 153 K (at 267 K for CsD_2PO_4)⁹⁴. The paraelectric phase is disordered the disorder being due to the short hydrogen bond which can be described in terms of statistical distribution of the proton on two off-center equivalent sites above T_c and an ordered asymmetric configuration below. In this proton ordering process the crystallographic center of inversion is lost and the $P2_1/m$ space group transforms to $P2_1$ while the number of molecules per unit cell ($Z = 2$) remains constant⁹³.

Vibrational study of this crystal also shows that the external vibrations of the paraelectric phase follow the C_{2h} factor group selection rules while the internal modes do not⁹⁵. In ferroelectric phase TO-LO splitting is observed for a number of internal and external vibrations.

There are 15 lattice modes of the paraelectric phase ($5A_g + 4B_g + 3A_u + 3B_u$): six R' and 6 T' vibrations are hydrogen bond motions while three T' ($2A_g + B_g$) modes involve motions of cations. Among $\nu OH \cdots O$ vibrations three $\nu OH \cdots O$ modes have been assigned at 234 (B_g, R'), 220 (A_u, R'), and 219 (A_g, R_b') cm^{-1} ⁴⁹. The last one appears the most interesting and will be discussed in some detail.

The $\nu OH \cdots O$ mode of A_g species becomes an A vibration in the ferroelectric phase and splits into a LO component at 249 cm^{-1} and a TO component at 205 cm^{-1} at 80 K (Figure 7). The relative splitting is about 20% and thus

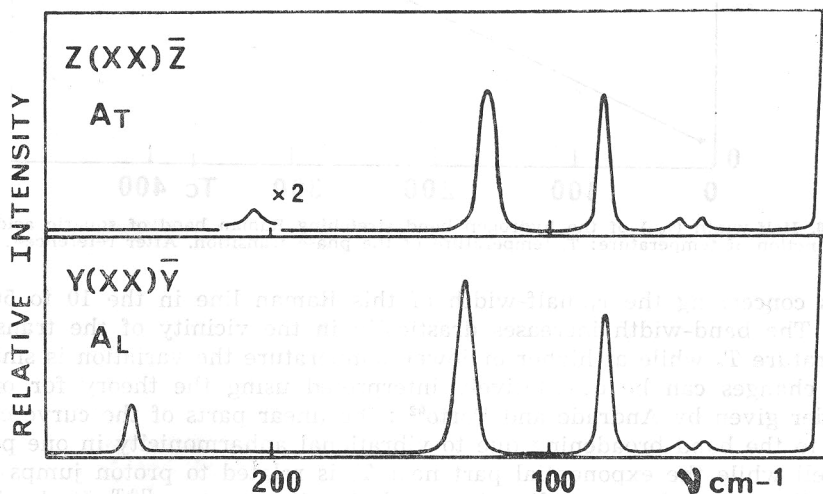


Figure 7. Low-frequency backward Raman scattering of CsH_2PO_4 single crystal at 80 K: $\alpha(XX)\bar{\alpha}$ geometry. After reference⁴⁹.

the largest of all vibrations of CsH_2PO_4 ; the splitting of the corresponding $\nu OD \cdots O$ mode is considerably smaller ($\sim 10\%$). The LO frequency is almost temperature insensitive while the TO frequency remains constant up to T_c but increases strongly from 205 to 220 cm^{-1} above T_c which is rather unusual behaviour for a lattice mode. The analogous TO frequency of CsD_2PO_4 on the other hand, does not vary under the same conditions. A possible explanation of such temperature dependence of this hydrogen bond stretching is that the hydrogen bond becomes stronger at higher temperature. In fact, the $O \cdots O$ distance of the short hydrogen bond shortens from 2.488 to 2.476 Å when going from the low- to the high-temperature phase⁹⁶ and the corresponding νOH frequencies decrease much more (from 2200 to 2100 cm^{-1}) than νOD frequencies (from 1870 to 1860 cm^{-1}) on heating the crystal to 300 K⁴⁹.

The temperature dependence of the half-width of these $\nu OH \cdots O$ and $\nu OD \cdots O$ Raman bands is also different: the slope of the $\nu 1/2$ versus temperature curve is much steeper for CsH_2PO_4 with a maximum value of 45 cm^{-1} than for CsD_2PO_4 with $\nu 1/2 = 15$ cm^{-1} . This difference may be related to

proton jumps along the OH··O and OD··O bonds and to different anharmonicity of the corresponding vibrations. It may be argued qualitatively that the activation energy which is roughly the height of the potential barrier of the double well potential, must be considerably higher for OD··O than for OH··O bond the former being about 0.022 Å longer⁹⁶. The corresponding correlation time, or tunnelling probability, and half-width are thus expected to be smaller for OD··O than for OH··O stretching band. A striking difference of the far-infrared ν OH··O and ν OD··O bands near 220 and 208 cm⁻¹, respectively is consistent with the above assumption⁴⁹.

REFERENCES

1. G. C. Pimentel and A. L. McClellan, *Ann. Rev. Phys. Chem.* **22** (1971) 347.
2. G. L. Hofacker, Y. Maréchal, and M. A. Ratner in: *The Hydrogen Bond*, P. Schuster, G. Zundel, and C. Sandorfy, North Holland, Amsterdam, Vol. **I**, (1976), p. 295.
3. D. Hadži and S. Bratos in: *The Hydrogen Bond*, P. Schuster G. Zundel, and C. Sandorfy, North Holland, Amsterdam, Vol. **II**, (1976) p. 613.
4. S. Bratos, J. Lascombe, and A. Novak in: *Molecular Interactions*, H. Ratajczak and W. J. Orville-Thomas, John Willey & Sons, (1980), p. 301.
5. Y. Maréchal in: *Molecular Interactions*, H. Ratajczak and W. J. Orville-Thomas, John Willey & Sons, (1980), po. 231.
6. G. C. Pimentel and A. L. McClellan, *The Hydrogen Bond*, W. F. Freeman, San Francisco, (1960), p. 132.
7. R. J. Jakobsen, J. W. Brasch, and Y. Mikawa, *Appl. Spectry.* **22** (1968) 641.
8. K. D. Möller and W. G. Rothschild, *Far-Infrared Spectroscopy*, Wiley-Interscience, New-York, (1971), p. 198.
9. J. L. Wood, in: *Spectroscopy and Structure of Molecular Complexes*, J. Yarwood; Plenum Press, London, (1973) p. 364.
10. I. G. Bonner and J. S. Kirby-Smith, *Phys. Rev.* **57** (1940) 1078.
11. R. C. Millikan and K. S. Pitzer, *J. Amer. Chem. Soc.* **80** (1958) 3515.
12. T. Miyazawa and K. S. Pitzer, *J. Amer. Chem. Soc.* **81** (1959) 74.
13. A. E. Stanevich, *Opt. Spectry.* **16** (1964) 243.
14. V. Ananthanarayan, *Spectrochim. Acta* **20** (1964) 197.
15. G. L. Carlson, R. E. Witkowski, and W. Fateley, *Spectrochim. Acta* **22** (1966) 1117.
16. G. Statz and E. Lippert, *Ber.* **71** (1967) 673.
17. S. G. W. Ginn and J. L. Wood, *J. Chem. Phys.* **46** (1967) 2735.
18. R. J. Jakobsen, Y. Mikawa, and J. W. Brasch, *Spectrochim. Acta* **23A** (1967) 2199.
19. Y. Mikawa, J. W. Brasch, and R. J. Jakobsen, *J. Mol. Spectry.* **24** (1967) 314.
20. M. Suzuki and T. Shimanouchi, *J. Mol. Spectry.* **28** (1968) 394.
21. M. Suzuki and T. Shimanouchi, *J. Mol. Spectry.* **29** (1969) 415.
22. D. Clague and A. Novak, *J. Mol. Structure*, **5** (1970) 149.
23. D. Clague and A. Novak, *J. Chim. Phys.* **67** (1970) 1126.
24. L. Colombo and K. Furić, *Spectrochim. Acta* **27A** (1971) 1773.
25. S. Meshitsuka, H. Takahashi, K. Higasi, and B. Schrader, *Bull. Chem. Soc. Japan* **45** (1972) 1664.
26. R. Foglizzo and A. Novak, *J. Chim. Phys.* **71** (1974) 1322.
27. W. G. Rothschild, *J. Chem. Phys.* **61** (1974) 3422.
28. J. de Villepin and A. Novak, *Spectrochim. Acta* **34A** (1978) 1009 and 1019.
29. J. de Villepin, D. Bougeard, and A. Novak, to be published.
30. C. Pigenet, G. Lucazeau, and A. Novak, *J. Chim. Phys.* **73** (1976) 141.
31. J. C. Lassègues, unpublished results.
32. S. Kishida and K. Nakamoto, *J. Chem. Phys.* **41** (1964) 1558.

33. R. F. Lake and H. W. Thompson, *Proc. Roy. Soc.* **A291** (1966) 839.
34. A. B. Dempster and G. Zerbi, *J. Chem. Phys.* **54** (1971) 3600.
35. P. T. T. Wong and E. Whalley, *J. Chem. Phys.* **55** (1971) 1830.
36. R. J. Jakobsen and J. W. Brasch, *Spectrochim. Acta* **21** (1965) 1753.
37. W. J. Hurley, I. D. Kuntz Jr., and G. E. Leroi, *J. Amer. Chem. Soc.* **88** (1966) 3199.
38. S. G. W. Ginn and J. L. Wood, *Spectrochim. Acta* **23A** (1967) 611.
39. G. Lichtfus and Th. Zeegers-Huyshens, *J. Mol. Structure* **9** (1971) 343.
40. N. Le Calvé, M-H. Limage, S. Parent, and B. Pasquier, *J. Chim. Phys.* **74** (1977) 917.
41. J. le Calvé, *J. Chim. Phys.* **67** (1970) 993.
42. D. Hadži and A. Novak, in: *International far-infrared and interferometry meeting*, Beckman, Geneva, 1968, p. 34.
43. A. Goypiron, J. de Villepin, and A. Novak, *Spectrochim. Acta* **31A** (1975) 805.
44. A. Novak, *Structure and Bonding*, **18** (1974) 177.
45. S. Nakashima and M. Balkanski, *Solid State Commun.* **19** (1976) 1225.
46. D. Bougeard and A. Novak, *Solid State Commun.* **27** (1978) 453.
47. G. Lucazeau and A. Novak, *J. Raman Spectry* **1** (1973) 573.
48. Y. Nakamoto, Y. A. Sarma, and K. Ogoshi, *J. Chem. Phys.* **34** (1965) 194.
49. B. Marchon and A. Novak, *J. Chem. Phys.* in press.
50. D. Hadži and B. Orel, *Spectrochim. Acta* **29A** (1973) 1745.
51. A. Novak, *J. Chim. Phys.* **69** (1972) 1615.
52. B. Orel and D. Hadži, *Chemica Scripta* **11** (1977) 102.
53. A. C. Pavia and P. A. Giguère, *J. Chem. Phys.* **52** (1970) 3551.
54. J. J. Rush, L. W. Schroeder, and A. J. Melveger, *J. Chem. Phys.* **56** (1972) 2793.
55. A. C. Legon, D. J. Millen, and S. C. Rogers, *Proc. Roy. Soc. London* **A370** (1980) 213.
56. J. W. Bevan, A. C. Legon, D. J. Millen, and S. C. Rogers, *Proc. Roy. Soc. London* **A370** (1980) 239.
57. R. K. Thomas and H. W. Thompson, *Proc. Roy. Soc. London*, **A316** (1970) 303.
58. D. J. Millen, *J. Mol. Structure* **45** (1978) 1.
59. R. K. Thomas, *Proc. Roy. Soc. London* **A322** (1971) 137.
60. J. E. Bertie and M. V. Falk, *Can. J. Chem.* **51** (1973) 1713.
61. V. Lorenzelli and A. Allemagne, *C. R. Acad. Sci.* **257** (1963) 2977.
62. A. Lautié and A. Novak, *Can. J. Spectry*, **17** (1972) 113.
63. C. Perchard and A. Novak, *J. Chem. Phys.* **48** (1968) 3079.
64. L. Colombo, *J. Chem. Phys.* **49** (1968) 4688.
65. L. Colombo, K. Furić, and D. Kirin, *J. Mol. Spectry* **39** (1971) 217.
66. L. Colombo, P. Bleckman, B. Schrader, R. Schneider, and Th. Plessler, *J. Chem. Phys.* **61** (1974) 3270.
67. D. Bougeard, N. Le Calvé, B. Saint-Roch, and A. Novak, *J. Chem. Phys.* **64** (1976) 5152.
68. D. Bougeard, A. Lautié, and A. Novak, *J. Raman Spectry*, **6** (1977) 80.
69. A. Lautié and A. Novak, *J. Chim. Phys.* **71** (1974) 415.
70. I. Harada and R. C. Lord, *Spectrochim. Acta* **23A** (1970) 611.
71. K. Itoh and T. Shimanouchi, *Biopolymers* **5** (1967) 921.
72. R. Foglizzo and A. Novak, *J. Chem. Phys.* **50** (1969) 5366.
73. R. Foglizzo and A. Novak, *J. Mol. Structure* **7** (1971) 205.
74. A. Lautié and A. Novak, *J. Chim. Phys.* **68** (1971) 1492.
75. W. C. Hamilton and J. A. Ibers, *Hydrogen bonding in solids*, W. A. Benjamin, Inc. New-York, (1968) p. 108.
76. P. Bosi, R. Tubino, and G. Zerbi, *J. Chem. Phys.* **59** (1973) 4578.
77. P. Bosi, G. Zerbi, and E. Clementi, *J. Chem. Phys.* **66** (1977) 3376.
78. S. Besnainou and D. L. Cummings, *J. Mol. Structure* **34** (1976) 131.
79. M. L. Batuev, *Izvest. Akad. Nauk. SSSR, Ser. Fiz.* **11** (1947) 336.
80. V. M. Chulanovski and S. D. Simova, *Dokl. Akad. Nauk SSSR* **68** (1949) 1033.
81. Y. Maréchal and A. Witkowski, *J. Chem. Phys.* **48** (1968) 3697.

82. S. Bratos, *J. Chem. Phys.* **63** (1975) 3499.
83. J. C. Lassègues and J. Lascombe, in: *Vibrational spectra and structure*, Ed. J. R. Durig, Elsevier, in press.
84. J. E. Bertie and D. J. Millen, *J. Chem. Soc.* (1965) 514.
85. J. C. Lassègues and P. V. Huong, *Chem. Phys. Lett.* **17** (1972) 444.
86. R. K. Thomas, *Proc. Roy. Soc. London*, **A344** (1975) 579.
87. F. Fillaux, *Chem. Phys.* **62** (1981) 287.
88. A. Novak, *J. Chim. Phys.* **72** (1975) 81.
89. A. Lautié and A. Novak, *Nature*, **216** (1967) 1202.
90. J. Feder, *Ferroelectrics*, **12** (1976) 71.
91. D. Semmingsen, *Acta Chem. Scand.* **27** (1973) 3961.
92. P. do R. Andrade and S. P. S. Porto, *Solid State Commun.* **14** (1974) 547.
93. B. C. Frazer, D. Semmingsen, W. D. Ellenson, and G. Shirane, *Phys. Rev.* **B20** (1979) 2745.
94. A. Levstik, R. Blinc, P. Kadaba, S. Čizikov, I. Levstik, and C. Filipič, *Solid State Commun.* **16** (1975) 1339.
95. B. Marchon, B. Pasquier, N. Le Calvé, A. Novak, M. Čopič, M. Zgonik, D. L. Fox, and B. B. Lavrenčič, *J. Chem. Phys.* **74** (1981) 5293.
96. D. Semmingsen and R. K. Thomas, unpublished results.

IZVLEČEK

Aleksander Novak

Medmolekulska nihanja vodikove vezi

Medmolekulska nihanja vodikove vezi $AH \cdots B$ opazimo v daljnem infrardečem delu spektra in blizu vzbujevalne črte v Ramanskem sipanju. Ta nihanja, posebno valenčno nihanje $\nu AH \cdots B$, so zanimiva, ker nam lahko med drugim dajo podatke o potencialnih konstantah $F_{H \cdots B}$ vodikove vezi in jih rabimo za računanje ravnovesnih konstant asociacije raznih kompleksov. Članek podaja štiri aspekte nihanj vodikove vezi. Prvi del obravnava vprašanja asignacije trakov raznim valenčnim (ν) in deformacijskim (δ in γ) nihanjem vodikove vezi, kriterije za asignacijo sistemov v plinskem, tekočem in zlasti v trdnem stanju in pri sklopitvi nihanj $\nu AH \cdots B$ in $\delta AH \cdots B$ z intramolekularnimi nihanji. Podrobneje se seznanimo z nihanji vezi $OH \cdots O$ karbonskih kislin, alkoholov, fenolov in kislih soli ter z nihanji vezi $NH \cdots X$ dušikovih baz in njihovih protoniranih derivatov. Več kot sto frekvenc $\nu AH \cdots B$ je zbranih v tabeli II. Drugi del se ukvarja s potencialnimi konstantami $F_{H \cdots B}$, z njihovimi izračuni in s korelacijami med frekvenco νAH in $F_{H \cdots B}$. Izkazuje se, da konstanta $F_{H \cdots B}$ ne odraža le vodikovo vez, ampak tudi druge, včasih enako pomembne, medmolekulske sile zvezane z dipoli, kvadrupoli in s silami zaradi prenosov naboja. Taki primeri so kvantitativno ocenjeni za kristale mravljične in brezvodne oksalne kisline. V tretjem delu je obravnavana vloga nihanj vodikove vezi pri določanju profila, tj. širine in strukture, pasu νAH . Ta nihanja nedvomno vplivajo na širino pasu, medtem ko je njihov vpliv na strukturo verjetno omejen na majhno število preprostih kompleksov v plinskem stanju. Zadnje poglavje presoja vlogo nihanj $\nu OH \cdots O$ v dinamiki faznih prehodov pri nekaterih ferroelektričnih kristalih, kot kvadratna kislina in CsH_2PO_4 , in analizira podatke, ki jih dobimo pri študiju ustreznih trakov v odvisnosti od temperature.